Published in final edited form as:
Arterioscler Thromb Vasc Biol. 2011 September ; 31(9): 2024–2034. doi:10.1161/ATVBAHA.111.232587.

Pericyte-Derived MFG-E8 Regulates Pathologic Angiogenesis

Sei-ichiro Motegi, **Wolfgang W. Leitner**, **Michael Lu**, **Yayoi Tada**, **Miklós Sárdy**, **Chuanjin Wu**, **Triantafyllos Chavakis**, and **Mark C. Udey**
Dermatology Branch (S.M., W.W.L., M.L., Y.T., M.S., C.W., M.C.U.) and Experimental Immunology Branch (T.C.), Center for Cancer Research, National Cancer Institute, NIH, Bethesda, Maryland, USA.

Abstract

Objective—MFG-E8 (lactadherin, SED1) is a secreted glycoprotein that has been previously implicated in enhancement of VEGF-dependent angiogenesis. Major sources of MFG-E8 *in vivo*, and precise mechanisms of MFG-E8 action remain undetermined. The objective of this study was to identify important sources of MFG-E8 *in vivo*, and further elucidate the role(s) of MFG-E8 in the regulation of angiogenesis.

Methods and Results—We utilized knockout mice and anti-MFG-E8 antibodies to study MFG-E8 function *in vivo*. In melanomas and in retinas of mice with oxygen-induced retinopathy, MFG-E8 colocalized with pericytes rather than endothelial cells, and platelet-derived growth factor receptor β (PDGFRβ)+ pericytes/pericyte precursors purified from tumors contained large amounts of MFG-E8 mRNA. Tumor- and retinopathy-associated angiogenesis was diminished in MFG-E8 knockout mice and pericyte coverage of neovessels was reduced. Inhibition of MFG-E8 production by 10T1/2 cells (surrogate pericyte/pericyte precursors) using small interfering (si)RNAs and short hairpin (sh)RNAs, or inhibition of MFG-E8 action with some anti-MFG-E8 antibodies, selectively attenuated migration *in vitro*. Significantly, the anti-MFG-E8 antibodies that inhibited 10T1/2 cell migration *in vitro* also inhibited pathologic angiogenesis *in vivo*.

Conclusions—These studies strongly implicate MFG-E8 in pericytes/pericyte precursor function, and indicate that MFG-E8-directed therapeutics may merit further development.

Keywords

MFG-E8; pericyte; angiogenesis; oxygen-induced retinopathy; melanoma

Pathologic neovascularization is an important component of several diseases, including cancer and proliferative retinopathies (both diabetic retinopathy and retinopathy of prematurity), and anti-angiogenic therapy is commonly used in patients with these

Correspondence to Mark C. Udey, Dermatology Branch, Center for Cancer Research, National Cancer Institute, NIH, 9000 Rockville Pike, Building 10, Room 12N238, Bethesda, MD 20802-1908, USA. Phone: (301) 496-2481; Fax: (301) 496-5370; udeym@mail.nih.gov.
Current affiliation for Y.T. is Department of Dermatology, Graduate School of Medicine, University of Tokyo, Tokyo, Japan.
Current affiliation for M.S. is Department of Dermatology and Allergology, Medical Center of the Munich University (LMU), Munich, Germany.
Current affiliation for T.C. is Division of Vascular Inflammation, Diabetes and Kidney, Department of Medicine and Institute of Phsyiology, Dreseden University of Technology, Dresden, Germany

Disclosures
None.

conditions. Most active agents act on endothelial cells (EC) via inhibition of vascular endothelial growth factor (VEGF) or VEGF receptor (VEGFR) tyrosine kinase signaling,[1,2] but supporting cells such as pericytes (PC) have also been targeted.[3–5] PC influence EC by producing proteins including VEGF and angiopoietin (Ang) 1, and these secreted growth factors promote EC survival, migration, proliferation and formation of branching vessels in vitro.[6–9] *In vivo*, PC regulate vessel structure and permeability.[6–9] EC contribute to this dialog by producing platelet-derived growth factor (PDGF) that enhances PC/PC precursor recruitment, proliferation and differentiation.[6–9] In mice, inhibition of PDGF/PDGF receptor β (PDGFRβ) signaling depletes PC from tumor-associated vessels in the Rip1-Tag2 pancreatic cancer model, leading to reduced angiogenesis and tumor growth, especially when combined with anti-VEGF therapy.[4] These data indicate that PC play an important role in tumor-related angiogenesis, and thus may represent a viable therapeutic target.

MFG-E8 (also lactadherin and SED1) is a secreted glycoprotein that was initially identified as a component of milk fat globules (MFG), and that is also produced by various phagocytes including tingible-body macrophages and follicular dendritic cells in splenic germinal centers, macrophages in peripheral lymph nodes, activated peritoneal macrophages, and immature dendritic cells, including epidermal Langerhans cells.[10–13] MFG-E8 is comprised of two N-terminal epidermal growth factor (EGF)-like domains, and two C-terminal discoidin-like domains (C1 and C2) that are homologous to blood coagulation factors V and VIII. One EGF-like domain (E2) contains an RGD consensus integrin-binding sequence, and MFG-E8 binds to αvβ3/5 integrins. The carboxy-terminal domains bind to negatively charged and oxidized phospholipids (like Factors V and VIII).[14] Because MFG-E8 binds avidly to phosphatidyl serine that is exposed on the surface of early apoptotic cells, MFG-E8 acts as an opsonin that targets apoptotic cells for uptake by αv integrin-expressing phagocytes.[10,15] This process has been reported to influence regulatory T cell development in B16 melanoma tumors[16] and to contribute to several other diseases including autoimmunity, mastitis, sepsis, atherosclerosis and Alzheimer's disease.[11,17–20] Interactions with αv integrins have also been previously implicated in regulation of angiogenesis and mammary gland branching.[21,22] Interactions mediated via the C1 domain of MFG-E8 are important for sperm-egg binding and enhancement of collagen turnover.[23,24]

With regard to angiogenesis, Silvestre and colleagues have previously reported that MFG-E8 enhanced revascularization in a mouse model of acute hind limb ischemia.[21] The angiogenesis-promoting activity of MFG-E8 was attributed to enhancement of VEGF-induced Akt phosphorylation and EC survival in an αvβ3/αvβ5 integrin-dependent manner, and EC were proposed to be the predominant source of MFG-E8. Our group subsequently demonstrated that MFG-E8 enhanced tumor-related angiogenesis and tumor growth in the Rip1-Tag2 mouse pancreatic tumor model, a model in which tumor progression is critically dependent on angiogenesis.[25] The source (or sources) of MFG-E8 in tumors was not determined and the mechanism by which MFG-E8 potentiated angiogenesis was not addressed. We have now additionally characterized the involvement of MFG-E8 in the regulation of angiogenesis in tumors, as well as in oxygen-induced retinopathy (OIR) in mice. Herein we demonstrate that PC/PC precursors are important sources of MFG-E8 *in vivo*, that MFG-E8 may enhance angiogenesis via actions on PC/PC precursors as well as EC, and that MFG-E8 can be effectively targeted with therapeutic benefit.

Materials and Methods

Detailed descriptions of materials and methods used in this study are available in the supplemental materials at http://atvb.ahajournals.org.

Mice

MFG-E8 knockout (KO) mice were generated as described previously[25] and backcrossed to C57BL/6 mice as described in the Online Data Supplement. Control animals were purchased from the NCI/Frederick Animal Production Program unless otherwise indicated.

Cells and Tumor Implantation Studies

B16F10 melanoma cells (Tumor Cell Repository of the NCI/Frederick Cancer Resaerch and Development Program) were implanted subcutaneously into syngeneic mice as indicated and tumors sizes (width × length) were determined with calipers. 10T1/2 cells were obtained from the ATCC.

Antibodies and Flow Cytometry

Monoclonal and polyclonal anti-mouse MFG-E8 antibody (Ab) were generated and characterized as described in the Online Data Supplement. Other monoclonal antibodies were obtained from commercial sources. Tumor cell subpopulations were obtained from single cell suspensions via preparative flow cytometry (BD FACSAria™ II Flow Cytometer (BD Biosciences)).

Immunofluorescence Microscopy and Image Analysis

Frozen sections from tumors were stained as described in the supplement and visualized with an AxioImager A1 conventional immunofluorescence microscope (Zeiss) or a LSM510 confocal laser-scanning microscope (Zeiss). Selected images were analyzed using Image J software.

Measurement of Vessel Permeability

Tumor vessel permeability was quantified by determining the amount of dye that extravasated after i.v. injection (Miles assay- see supplement).[26]

Assessment and Treatment of Oxygen-Induced Retinopathy-Associated Angiogenesis

Angiogenesis associated with oxygen-induced retinopathy (OIR) was studied in neonatal MFG-E8 knockout and littermate control mice as previously described,[27] and neovascularization was quantified as described in the supplementary materials. Mice were exposed to 75% O_2 from P7–P12 and 20% O_2 from P12–P17. In treatment studies, rabbit anti-MFG-E8 pAb, mouse anti-MFG-E8 mAb and appropriate control proteins were injected i.p. (50 μg per injection) on days P12, 14 and 16 (normoxic period). On day P17, retinal neovascularisation was quantified.

MFG-E8 Knockdown Experiments and Quantification of MFG-E8 mRNA and Protein

MFG-E8 production by 10T1/2 cells was inhibited by small interfering (si)RNAs and short hairpin (sh)RNAs as described in the supplementary materials. MFG-E8 mRNA levels were determined using quantitative RT-PCR and MFG-E8 protein production was quantified by ELISA (see supplement).

10T1/2 cell migration, proliferation and differentiation studies

PDGF-dependent 10T1/2 cell migration, proliferation, and TGF-β1-dependent differentiation was assessed as described in the supplemental materials. Migration assays were carried out in transwell plates.

Statistics

P values were calculated using the Student's *t*-test (two-sided) or by analysis of one-way ANOVA followed by Bonferroni's post test as appropriate. Survival differences were calculated using a log-rank test. Error bars represent standard errors of the mean, and numbers of experiments (n) are as indicated.

Results

Production of MFG-E8 by Tumor Vessel-Associated Pericytes

We previously reported that, in the Rip1-Tag2 model of pancreatic β-cell tumorigenesis, MFG-E8 was predominantly vessel-associated, and we suggested, based on preliminary immunfluorescence studies, that MFG-E8 appeared to colocalize with PC.[25] To definitively address the origin, and to gain insights into the mode of action, of MFG-E8 in tumors, we developed improved reagents and carried out additional experiments. High-titer, affinity-purified, mono-specific anti-MFG-E8 polyclonal Ab (pAb) were raised in rabbits, purified, characterized as described in the Supplemental Methods and Figure 4A, and then utilized to localize MFG-E8 protein in tissue sections of rapidly-growing, non-necrotic (1 cm diameter) B16F10 melanoma tumors that had been implanted subcutaneously in the flanks of C57BL/6 mice. The intensity of staining that we observed was much greater than that seen with the mouse anti-mouse MFG-E8 mAb that we previously described,[25] allowing for more precise localization of MFG-E8 protein in tumors *in situ* using confocal laser immunofluorescence microscopy. Double staining of tumor sections for MFG-E8 and the EC marker CD31 revealed that MFG-E8 staining occurred primarily around, and in close proximity to, CD31+ blood vessels (Figure 1A, and Supplemental Figure IA and IB (arrows)). Interestingly, the perivascular distribution of MFG-E8 protein was primarily external to EC and was much more coincident with PDGFRβ+ and NG2+ PC (Figure 1A and Supplemental Figure IB, IC and ID). Note that, in B16 tumors, there was almost complete correspondence of PDGFRβ and NG2 perivascular staining (Supplemental Figure ID). Analysis of digital images with Image J revealed that whereas only 27% of the CD31+ area overlapped with perivascular MFG-E8-specific immunofluorescence, 66% of the PDGFRβ and 54% of the NG2 staining colocalized with MFG-E8 (Figure 1B). These results suggested that, in established B16 tumors, only a minority of MFG-E8 protein was melanoma cell-derived and, further, that PDGFRβ+ NG2+ PC might be a more important source of MFG-E8 than ECs.

However, in addition to MFG-E8-producing perivascular cells (arrows in Supplementary Figure IB, IE and IF), we identified small numbers of PDGFRβ+ MFG-E8+ stromal cells that were not obviously associated with blood vessels in B16 tumors (see arrowheads in Supplementary Figure 1E). We also detected PDGFRβ+ MFG-E8- spindle cells near the periphery of tumors (see arrowheads in Supplementary Figure 1F). The identities of these minor subpopulations are unknown, but the former may represent PC precursors and the latter may be fibroblasts. Somewhat surprisingly, we did not observe MFG-E8 positive leukocytes (CD45+) or macrophages (CD68+) in melanomas (data not shown).

To test the hypothesis that intra-tumoral PC produced large amounts of MFG-E8, we assessed the levels of mRNA encoding MFG-E8 in tumor cell subpopulations derived from B16 melanomas. To accomplish this, we prepared single cell suspensions from tumors and utilized preparative flow cytometry to purify leukocytes (white blood cells (WBC); CD45+, CD31−), EC (CD45−, CD31+), PC (CD45−, CD31−, PDGFRβ+) and cells enriched B16 melanoma cells (CD45−, CD31−, PDGFRβ−) (Figure 1C). Note that we cannot exclude contamination of tumor cell fraction with lineage marker-negative stromal cells. We also cannot rule out the possibility that CD45−, CD31−, PDGFRβ+ cells include small number of non-PC. RNA was extracted from unsorted and sorted cells, and MFG-E8 mRNA levels

were determined using quantitative real-time PCR. Relative to unfractionated tumor cells (MFG-E8 mRNA abundance=1), levels of MFG-E8 mRNA were decreased in melanoma cells (0.7) and WBC (0.4), and increased in EC (1.3) and PC (3.9) (Figure 1D). These results, considered in conjunction with our *in situ* localization studies, indicate that PC can produce MFG-E8 in tumors and that, on a per cell basis, PC have a greater capacity to produce MFG-E8 protein than all other tumor-associated cells.

Influence of Host-Derived MFG-E8 on Tumor-Associated Vessels and Melanoma Growth

Because MFG-E8 protein localized primarily around tumor blood vessels (Figure 1 and Supplemental Figure I), we assessed the involvement of MFG-E8 in development and function of tumor vessels and tumor growth. The vascularity of B16 melanomas growing in the subcutis of C57BL/6 MFG-E8 KO mice was ~50% of that in tumors growing in wild type (WT) mice as assessed by quantifying the relative areas of CD31 immunofluorescence staining using Image J (Figure 2A and 2B and Supplemental Figure II). Quantification of tumor vessel-associated PC using an analogous approach revealed a significantly reduction in KO tumors, and the level of PC coverage which was assessed by PC/EC ratio in KO tumors was also significantly reduced. (Figure 2A and 2B and Supplemental Figure II). Consistent with this finding, vessel permeability (detected via quantification of extravasated Evan's blue dye) was increased in tumors in KO mice (Figure 2C). Because the vascularity of B16 melanomas in MFG-E8 KO mice was reduced by ~50%, the permeability of vessels that formed must be dramatically increased relative to vessels in tumors in control mice.

To determine the impact of decreased tumor vascularity, we implanted B16 melanoma cells into MFG-E8 KO and WT mice and measured tumor progression. Tumor growth in KO mice was significantly inhibited compared with that in WT mice, and the survival of tumor-bearing KO mice was extended (Figure 2D). Quantification of cell proliferation after staining with Ki-67 revealed that tumor cell proliferation in KO mice was inhibited by ~30% compared with that in WT mice (Figure 2E). We did not detect significant Ki-67 staining in CD31+ EC in melanomas and also did not detect differences in this parameter in tumors in WT and MFG-E8 KO mice. Apoptotic tumor cell frequencies (terminal deoxynucleotidyl transferase-mediated dUTP nick end labeling (TUNEL)+ areas in tumors) were also equivalent in tumors in WT and MFG-E8 KO mice (Figure 2E) and there were no differences in the numbers of TUNEL and CD31 double-positive cells in tumors in WT and KO mice (data not shown).

To assess the possibility that MFG-E8 protein that was produced by malignant cells might elicit a tumor-reactive immune response in MFG-E8 KO mice and that this might explain the attenuated tumor growth that was observed, we assessed B16 tumor growth in MFG-E8 KO and WT mice that had been treated with lymphocyte-depleting anti-CD4 (GK1.5) and/or anti-CD8 (2.43) mAb. Although anti-CD4 mAb treatment delayed tumor growth in both WT and MFG-E8 KO mice, differences between WT and KO mice persisted after treatment with either of the mAb alone or in combination (Supplemental Figure III). These results indicate that it is unlikely that anti-MFG-E8 immunity was responsible for delayed tumor growth in MFG-E8 KO mice, and suggest that the effect that we observed reflects a role for MFG-E8 in the regulation of angiogenesis.

Accumulation and Distribution of MFG-E8 in Melanomas in Wild Type and MFG-E8 Knockout Mice

The relative importance of malignant melanoma cells as a source of MFG-E8 in tumors was additionally analyzed by localizing MFG-E8 protein in B16 tumors growing in MFG-E8 KO mice via immunofluorescence microscopy. As expected, we observed much less intense MFG-E8-specific staining in tumors in KO mice than in WT mice (Figure 3). Interestingly,

however, the perivascular staining pattern that we observed in tumors in WT mice also predominated in MFG-E8 KO mice (Figure 3B). These results indicate that although most of the MFG-E8 protein that is present in tumors is derived from non-malignant cells (predominantly PC and EC), tumor cells also produce MFG-E8. Furthermore, even melanoma cell-derived MFG-E8 protein accumulates in areas where PC localize.

MFG-E8 and Susceptibility to Oxygen-Induced Retinopathy

To determine if MFG-E8 modulated angiogenesis only in tumors, or if this effect was more general, we next characterized the involvement of MFG-E8 in pathologic neoangiogenesis associated with oxygen-induced retinopathy (OIR) in mice. This condition mimics retinopathy of prematurity, is thought to model some aspects of diabetic retinopathy and is a non-tumor experimental system in which PC function can be studied in detail.[27] In the OIR model, post-natal day 7 (P7) pups are exposed to 75% oxygen for 5 days (P7–P12), and then returned to room air until P17 (when experiments are terminated). Exposure of neonatal mice to hyperoxia (75% O_2) leads to regression of retinal vessels. The relative retinal hypoxia that ensues when mice are placed in a normoxic (20% O_2) atmosphere induces neovascularization. Neovascularization can be readily quantified and anti-angiogenic interventions can be attempted during the P12–P17 “hypoxic” period.

In normal retinal whole-mounts from WT mice, most MFG-E8 colocalized with PDGFRβ+ and NG2+ PC while some MFG-E8 was CD68+ macrophage-associated (Figure 4A). The lack of staining of retinas from MFG-E8 KO mice confirms the high specificity of the anti-MFG-E8 pAb that we generated (Figure 4A). In mice subjected to OIR, numerous pathological neoangiogenic tufts were observed at P17 as expected (Figure 4B, arrows). These tufts were encased with PDGFRβ+ PC and were coated with MFG-E8 protein (Figure 4B). Scattered CD68+, MFG-E8+ macrophages were more numerous in these preparations than they were in retinas from untreated mice (data not shown), and some of these macrophages were located in close proximity to the angiogenic tufts (Figure 4B). We compared neovascularization in the retinas of WT and MFG-E8 KO mice in the OIR model, and determined that the reponse was blunted considerably in MFG-E8-deficient animals (Figure 4C and Supplemental Figure IV). Quantification of retinal vascularity using a standard morphometric approach confirmed this, and also revealed that heterozygous mice could not be distinguished from WT mice (Figure 4D). These results indicate that MFG-E8 derived from PC/PC precursors, and perhaps macrophages, promotes neovascularization in the OIR mouse model.

Cell Autonomous Actions of C3H 10T1/2 cell-Derived MFG-E8

Previous reports demonstrated that MFG-E8 potentiates VEGF action on EC.[21] The striking colocalizaton of MFG-E8 with PC that we observed suggested that PC-derived MFG-E8 might also act on PC. To test this hypothesis, we utilized the C3H 10T1/2 cells as surrogates PC/PC precursors in *in vitro* studies. 10T1/2 cells express the PC markers smooth muscle actin (SMA), NG2, desmin, and PDGFRβ[28,29] and they have previously been demonstrated to promote formation of cord-like structures when cocultured with bovine EC, suggestive of PC-like function,[30] and to be PDGF-responsive.[28,31] We confirmed that 10T1/2 cells produced both MFG-E8 mRNA and protein using quantitative RT-PCR and ELISA, respectively, and determined that 10T1/2 cells expressed 25-fold more MFG-E8 mRNA than B16 melanoma cells (Supplemental Figure V, A and B).

To examine the functional consequences of MFG-E8 production by 10T1/2 cells, we manipulated MFG-E8 mRNA accumulation and protein production with retroviruses encoding shRNAs that target MFG-E8 mRNA as well as corresponding siRNAs. MFG-E8 siRNAs inhibited mRNA and protein expression in 10T1/2 cells by 70–80% depending on

the sequence of the siRNA and the experiment (Supplemental Figure V, B and Supplemental Figure VI, A). Similar levels of inhibition were obtained with some, but not all, shRNAs (Supplemental Figure VII, A). In initial experiments, we tested the ability of 10T1/2 cells that had been transfected with siRNAs, or infected with retroviruses producing MFG-E8 and control shRNAs, to close "wounds" in cell monolayers in "scratch" assays. We observed that 10T1/2 cells that produced less MFG-E8 migrated more slowly than cells that produced normal amounts of MFG-E8, and that exogenous MFG-E8 could restore the migratory capacity of 10T1/2 cells with diminished MFG-E8 production (Supplemental Figure VI, B and Supplemental Figure VII, B).

Because EC-derived PDGF-B and PDGF-B/PDGFRβ signaling is critical for PC/PC progenitor cell recruitment during angiogenesis,[6–9] the involvement of MFG-E8 in PDGF-stimulated 10T1/2 cell migration was also studied using a transwell migration assay. After confirming that 10T1/2 cells expressed PDGFRβ by immunofluorescence staining, flow cytometry and RT-PCR (data not shown), we depleted MFG-E8 mRNA and protein in 10T1/2 cells and assessed PDGF-induced cell migration. In these experiments, MFG-E8 mRNA expression in MFG-E8 siRNA-transfected cells was inhibited by 55–70% relative to that in control siRNA-transfected cells (Figure 5A) and the ability of 10T1/2 cells depleted of MFG-E8 by RNA interference to migrate was also markedly inhibited (Figure 5B). In addition, as we observed in the "scratch assays" (see above), adding recombinant MFG-E8 into the medium reversed the migration inhibitory effects of MFG-E8 mRNA depletion (Figure 5B). These results strongly implicate 10T1/2-derived MFG-E8 as an autocrine regulator of cell migration.

We next examined the influence of anti-MFG-E8 Ab on PDGF-induced cell migration to determine if MFG-E8 might be a relevant therapeutic target. PDGF-induced 10T1/2 cell migration was inhibited by rabbit anti-MFG-E8 pAb that recognized the N-terminus of MFG-E8, and by inhibitory anti-αv integrin mAb to similar extents and the combination of anti-MFG-E8 and anti-αv integrin Ab was no more inhibitory than either Ab alone (Figure 5C). Addition of recombinant MFG-E8 reversed the inhibition caused by anti-MFG-E8 pAb, but not that due to anti-αv integrin mAb (Figure 5D). Mouse anti-MFG-E8 mAb B10C7 that recognized the RGD motif in the E2 domain (or a nearby epitope) also inhibited PDGF-induced 10T1/2 cell migration like anti-MFG-E8 pAb, whereas several other mAb were less effective (C1 domain-reactive mAb B18A9 and 1H6) or were ineffective (B1F10, a mAb reactive with an epitope in the E1, E2 or L domains) (Figure 5E). Both rabbit anti-MFG-E8 pAb and mouse anti-MFG-E8 mAb B10C7 inhibited cell migration in a dose-dependent manner, with maximal (~50%) inhibition occurring at 20–50 μg/ml for each Ab (Supplemental Figure VIII). In aggregate, these results suggest that MFG-E8 enhances 10T1/2 cell migration via binding to αv integrin on the surfaces of 10T1/2 cells, and that MFG-E8 may be the major 10T1/2 cell-derived αv integrin ligand that is involved in migration. The lesser, but also significant, inhibition that we observed with anti-MFG-E8 mAb B18A9 and 1H6 suggest that the C1 domain might also contribute to cell migration, perhaps by tethering MFG-E8 to the extracellular matrix.[24]

To determine if effects of MFG-E8 on 10T1/2 cell migration were secondary to global alterations in cell physiology, we assessed PDGF-BB and serum-induced proliferation in control and MFG-E8 siRNA-treated 10T1/2 cells. Data depicted in Supplemental Figure IX failed to document altered cell growth in MFG-E8 knockdown cells. We also sought to determine if MFG-E8 might regulate TGFβ1-induced 10T1/2 cell differentiation. TGF-β1 induces 10T1/2 cells to acquire characteristics of the smooth muscle cell (SMC)/PC lineage, and TGF-β1 is required for formation of capillary-like structures by EC and 10T1/2 cells.[28,30] As previously reported,[28] TGF-β1 induced αSMA expression in 10T1/2 cells (Supplemental Figure X). TGF-β induced αSMA expression by 10T1/2 cells was not altered

by MFG-E8 knockdown using siRNA, or anti-MFG-E8 pAb treatment (Supplemental Figure X). In aggregate, these results suggest that MFG-E8 regulates PC/PC precursor migration rather than proliferation or differentiation.

Inhibition of Oxygen-Induced Retinopathy by Anti-MFG-E8 Antibody

The OIR mouse model has previously been used to test several anti-angiogenic agents that are now widely used in the clinic or are in development, including agents that target VEGF/VEGF receptor signaling and integrin antagonists.[32–35] Having demonstrated that anti-MFG-E8 Ab could inhibit 10T1/2 cell migration *in vitro* and that neoangiogenesis in the OIR model was attenuated in MFG-E8 KO mice, we characterized the activities of anti-MFG-E8 Ab in the OIR model *in vivo*. We administered anti-MFG-E8 Ab that inhibited 10T1/2 cell migration *in vitro* to neonatal mice during the normoxic period (50 μg of Ab or control IgG injected i.p. on P12, P14 and P16) and quantified angiogenesis on P17. We determined that anti-MFG-E8 Ab inhibited pathologic neoangiogenesis, and observed that the relative potencies of the various reagents were similar in the *in vitro* and the *in vivo* assays (Figure 6). Interestingly, the magnitude of maximal inhibition of angiogenesis that we observed (~50%) was very similar to the degree of OIR attenuation that occurred in MFG-E8 KO mice. These results suggest that, in experimental animals, anti-MFG-E8 Ab can completely inhibit this aspect of MFG-E8 function, and that analogous agents may have therapeutic potential in patients.

Discussion

MFG-E8 is a glycoprotein that has multiple domains and binds to multiple ligands.[36–39] At this juncture, MFG-E8 has been implicated in a number of mouse models that have relevance to several important human diseases,[18–20,24,25,40] and in normal physiology as well.[17,22,23,41] Because MFG-E8 is secreted, and thus does not necessarily remain associated with the cells that produce it, and because MFG-E8 is produced by a variety of cells, determining where MFG-E8 is produced *in vivo* and how it acts is not trivial. This problem is additionally challenging because MFG-E8 production can be regulated. Thus, cells that produce MFG-E8 in the setting of stress or injury,[42] may or may not produce significant amounts of protein at baseline. The pleiotropic effects of MFG-E8 may also relate, at least in part, to the fact that the αvβ3 and αvβ5 integrins are the best characterized cell surface receptors for MFG-E8. These integrins are widely distributed, are promiscuous with regard to the extracellular matrix proteins that they bind to, and are important regulators of a number of biological activities that are basic and required for normal function of many cells (eg. migration, survival and proliferation).

We identified PDGFRβ+ PC and/or PC precursors as a major source of MFG-E8 in B16 melanoma tumors. Using a newly developed anti-MFG-E8 pAb that is much more sensitive than the mAb that was used in a previous report from our group,[25] we determined that MFG-E8 accumulation in tumors was primarily perivascular and that MFG-E8 staining co-localized with PC more than with EC. We also found that amounts of MFG-E8 mRNA in PDGFRβ+ PC/PC precursors and EC from tumors exceeded those in malignant cells and infiltrating WBC, and that MFG-E8 mRNA levels were 3-fold higher in PC/PC precursors than in EC. Finally, we observed much less intense staining of MFG-E8 in tumors growing in MFG-E8 KO mice than in WT mice. We conclude that in untreated B16 tumors, PC/PC precursors and EC are likely to be the most relevant sources of MFG-E8. These results are consistent with and extend the results of previous studies from our group and from other groups in which MFG-E8 was detected in association with adventitial microvessels, vascular smooth muscle cells in the media of the aorta, some luminal EC and PC.[19,21,25,41,43]

Although MFG-E8 staining was drastically reduced in B16 tumors growing in MFG-E8 KO mice, the perivascular staining pattern that we observed in tumors in WT mice also predominated in tumors in MFG-E8 KO mice. This indicates that MFG-E8 that was secreted by malignant cells continued to accumulate near PC. In normal blood vessels, PC and EC are surrounded by basement membrane that contains laminin, collagen type 4, nidogen and heparin sulfate proteoglycans.[6–8] We also detected perivascular laminin and collagens type 1 and 4 in B16 tumors in close proximity to PC (not shown). It has been demonstrated that MFG-E8 binds to collagen type 1 via the C1 domain,[24] providing a plausible explanation for its distribution in tumors.

Assessment of vascular structures in B16 tumors in control and MFG-E8 KO mice revealed significant differences that were consequential. Vessel density and PC coverage were reduced, and vascular permeability was increased in tumors in MFG-E8 KO mice. These alterations were associated with decreased malignant cell proliferation and delayed tumor growth. The involvement of MFG-E8 in B16 tumor growth has been studied previously,[16,40,42] but the experimental approaches that were used differed from those that we utilized. The previously published studies clearly indicate that MFG-E8 can have an immunomodulatory role when incorporated into melanoma cell-based vaccines, that MFG-E8 can enhance tumorigenesis when overexpressed in malignant cells, and that MFG-E8 production by malignant cells (including B16 cells) is increased by exposure to cytotoxic agents. We did not overexpress MFG-E8 in B16 cells and did not identify an important role for T cell immunity in attenuation of melanoma growth in MFG-E8 KO mice. We believe that our results implicating MFG-E8 in regulation of tumor vascularity are complementary to those that have previously been published[16,40,42] rather than inconsistent with them, reflecting the multiple and varied functional activities of this protein.

The concept that PC/PC precursor-derived MFG-E8 is important in pathologic angiogenesis is additionally supported by our studies in the OIR model. We determined that neovascular tufts were ensheathed with PC and coated with MFG-E8 in retinal whole-mounts, and that neoangiogenesis was markedly inhibited in MFG-E8 KO mice. Several previous studies examined the role of PC in OIR. NG2-deficient mice exhibited decreased PC/EC ratios in retinal neovascular tufts and decreased neovascularization in OIR.[44] In contrast, PDGF-B heterozygous mice, which also exhibit reduced PC coverage of retinal blood vessels showed increased neovascularization in OIR.[45] Although we could not quantify PC coverage in retinal vessels in our OIR studies, there is an apparent unresolved contradiction between these latter results and our results. Previous studies documented that microglia/macrophages were increased in the retinas of mice with OIR.[46] We also observed scattered macrophages, some in close approximation to neoangiogenic tufts, in OIR, and most of these CD68+ cells also expressed MFG-E8. Thus, our results clearly indicate that MFG-E8 regulates neoangiogenesis in OIR, and suggest that both PC and macrophages may be relevant sources.

A previous study reported that MFG-E8 promoted ischemia-induced angiogenesis and demonstrated that MFG-E8 enhanced VEGF-induced Akt phosphorylation and proliferation in EC via binding to αvβ3/5-integrins.[21] The striking colocalization of MFG-E8 with PC/PC precursors that we observed led us to hypothesize that MFG-E8 might act on PC/PC precursors as well as on EC. We studied C3H 10T1/2 cells as surrogates for PC/PC precursors. Derived from mouse embryos almost 40 years ago, 10T1/2 cells have been variously termed fibroblasts, PC-like cells, mesenchymal stromal cells, mesenchymal precursor cells, smooth muscle precursor cells and mesenchymal stem cells.[28–30,47–51] Although their precise relationship to normal PC is uncertain, 10T1/2 cells and PC share some surface characteristics, are both capable of influencing EC characteristics and each exhibit multilineage potential under some circumstances. We utilized 10T1/2 cells in the

experiments described herein because they produce MFG-E8, they were known to be PDGF-responsive (like PC) and they could be readily propagated and manipulated.

We observed that depletion of MFG-E8 from 10T1/2 cells by RNA interference markedly inhibited basal and PDGF-induced migration, and that adding recombinant MFG-E8 reversed these effects. We also determined that 10T1/2 cell migration was inhibited by rabbit anti-MFG-E8 pAb and mouse anti-MFG-E8 mAb (B10C7) that recognized the N-terminus of MFG-E8, and by inhibitory anti-αv integrin Ab to similar extents and that the combination of anti-MFG-E8 and anti-αv Ab was no more active than either alone. Interestingly, inhibition of MFG-E8 production or action did not attenuate 10T1/2 cell proliferation or obviously alter 10T1/2 cell differentiation. Thus, MFG-E8 may exert some of its proangiogenic effects by facilitating recruitment of PC and/or PC precursors to perivascular locations where they can support EC function.

Our results suggest that MFG-E8 enhances 10T1/2 cell migration via binding to αv integrins on the cell surfaces, and that (at least *in vitro*) MFG-E8 is an important autocrine αv ligand. Cell movement requires synergy between PDGF-and integrin-mediated signaling,[52] and we speculate that MFG-E8 facilitates cell migration by promoting this interaction. However, 10T1/2 cell migration was also inhibited to some extent by mouse anti-MFG-E8 mAb (B18A9 and 1H6) that recognize the C-terminus of MFG-E8. It has previously been reported that MFG-E8 enhanced the migration of mouse intestinal epithelial cells *in vitro* and *in vivo*.[53] This effect has been attributed to MFG-E8-phosphatidyl serine binding and resulting cytoskeletal reorganization, but the C-terminus of MFG-E8 also has other ligands. A recent study indicated that the C1 domain of MFG-E8 mediates binding and uptake of collagen type 1.[24] We detected collagen type 1 production by 10T1/2 cells *in vitro*, documented pericellular collagen deposition by immunofluorescence staining (unpublished observations), and we thus propose that binding of MFG-E8 to collagen type 1 via the C1 domain and engagement of αv integrins via the E2 domain of MFG-E8 may facilitate PDGF-induced 10T1/2 cell migration. Although the mechanism by which this may occur remains to be elucidated, cooperation between αv-integrins and growth factor receptors with tyrosine kinase activity is known to occur.[54]

Finally, we demonstrated that selected mAb and pAb that reacted with MFG-E8 and that were potent inhibitors of 10T1/2 cell migration *in vitro*, also inhibited angiogenesis *in vivo*. Ab that recognized the E1 and E2 domains (pAb) or an RGD-dependent epitope in the E2 domain of MFG-E8 (mAb B10C7) were effective inhibitors of OIR, whereas the mAb reactive with C-terminal domains were not. We conclude that PC/PC precursors are important sources of MFG-E8 *in vivo*, that PC/PC precursor-derived MFG-E8 promotes pathologic neoangiogenesis in several settings, and that MFG-E8 may enhance angiogenesis via actions on PC or PC precursors as well as EC. Our results also indicate that MFG-E8 is a relevant therapeutic target in several important disease models characterized by unwanted neoangiogenesis, and suggest that Abs that react with the N-terminus (especially the RGD sequence-containing E2 domain) may be particularly interesting. Extrapolating our results to patients, anti-human lactadherin (MFG-E8) Ab that bind to the single N-terminal EGF-like domain that contains the integrin binding site may warrant deliberate development. Ab with this characteristic may represent useful therapeutics when used alone or in conjunction with other agents (including other anti-angiogenic agents) in the treatment of diseases such as diabetic retinopathy or cancer.

Supplementary Material

Refer to Web version on PubMed Central for supplementary material.

Acknowledgments

We thank Dr. William G. Telford, Veena Kapoor, and Nga Voong (Experimental Transplantation & Immunology Branch, CCR, NCI) for assistance with cell sorting, Dr. Matina Economopoulou (Experimental Immunology Branch, CCR, NCI) for help with the whole-mount staining of retina and OIR studies, and Olga Milgrom and Mallorie Heneghan for performing mouse husbandry and genotyping.

Sources of Funding

This work was supported by the Intramural Program of NIH, Center for Cancer Research, National Cancer Institute (to M.C.U.). S.M. was supported, in part, by project grants from the Japan Foundation for Aging and Health, and a Japan Society for Promotion of Science (JSPS) Research Fellowship for Japanese Biomedical and Behavioral Researchers at NIH.

References

1. Backer MV, Hamby CV, Backer JM. Inhibition of vascular endothelial growth factor receptor signaling in angiogenic tumor vasculature. Adv Genet. 2009; 67:1–27. [PubMed: 19914448]
2. Schlingemann RO, Witmer AN. Treatment of retinal diseases with VEGF antagonists. Prog Brain Res. 2009; 175:253–267. [PubMed: 19660661]
3. Ostman A, Heldin CH. PDGF receptors as targets in tumor treatment. Adv Cancer Res. 2007; 97:247–274. [PubMed: 17419949]
4. Bergers G, Song S, Meyer-Morse N, Bergsland E, Hanahan D. Benefits of targeting both pericytes and endothelial cells in the tumor vasculature with kinase inhibitors. J Clin Invest. 2003; 111:1287–1295. [PubMed: 12727920]
5. Timke C, Zieher H, Roth A, Hauser K, Lipson KE, Weber KJ, Debus J, Abdollahi A, Huber PE. Combination of vascular endothelial growth factor receptor/platelet-derived growth factor receptor inhibition markedly improves radiation tumor therapy. Clin Cancer Res. 2008; 14:2210–2219. [PubMed: 18381963]
6. Diaz-Flores L, Gutiérrez R, Madrid JF, Díaz-Flores L, Gutiérrez R, Madrid JF, Varela H, Valladares F, Acosta E, Martín-Vasallo P, Díaz-Flores L Jr. Pericytes. Morphofunction, interactions and pathology in a quiescent and activated mesenchymal cell niche. Histol Histopathol. 2009; 24:909–969. [PubMed: 19475537]
7. Armulik A, Abramsson A, Betsholtz C. Endotherial/Pericyte Interactions. Circ Res. 2005; 97:512–523. [PubMed: 16166562]
8. Gaengel K, Genové G, Armulik A, Betsholtz C. Endothelial-mural cell signaling in vascular development and angiogenesis. Arterioscler Thromb Vasc Biol. 2009; 29:630–638. [PubMed: 19164813]
9. Chantrain CF, Henriet P, Jodele S, Emonard H, Feron O, Courtoy PJ, DeClerck YA, Marbaix E. Mechanism of pericyte recruitment in tumor angiogenesis: A new role for metalloproteinases. Eur J Cancer. 2006; 42:310–318. [PubMed: 16406506]
10. Hanayama R, Tanaka M, Miwa K, Shinohara A, Iwamatsu A, Nagata S. Identification of a factor that links apoptotic cells to phagocytes. Nature. 2002; 417:182–187. [PubMed: 12000961]
11. Hanayama R, Tanaka M, Miyasaka K, Aozasa K, Koike M, Uchiyama Y, Nagata S. Autoimmune disease and impaired uptake of apoptotic cells in MFG-E8-deficient mice. Science. 2004; 304:1147–1150. [PubMed: 15155946]
12. Miyasaka K, Hanayama R, Tanaka M, Nagata S. Expression of milk fat globule epidermal growth factor 8 in immature dendritic cells for engulfment of apoptotic cells. Eur J Immunol. 2004; 34:1414–1422. [PubMed: 15114675]
13. Kranich J, Krautler NJ, Heinen E, Polymenidou M, Bridel C, Schildknecht A, Huber C, Kosco-Vilbois MH, Zinkernagel R, Miele G, Aguzzi A. Follicular dendritic cells control engulfment of apoptotic bodies by secreting Mfge8. J Exp Med. 2008; 205:1293–1302. [PubMed: 18490487]
14. Raymond A, Ensslin MA, Shur BD. SED1/MFG-E8: a bi-motif protein that orchestrates diverse cellular interactions. J Cell Biochem. 2009; 106:957–966. [PubMed: 19204935]

15. Asano K, Miwa M, Miwa K, Hanayama R, Nagase H, Nagata S, Tanaka M. Masking of phosphatidylserine inhibits apoptotic cell engulfment and induces autoantibody production in mice. J Exp Med. 2004; 200:459–467. [PubMed: 15302904]
16. Jinushi M, Nakazaki Y, Dougan M, Carrasco DR, Mihm M, Dranoff G. MFG-E8-mediated uptake of apoptotic cells by APCs links the pro- and antiinflammatory activities of GM-CSF. J Clin Invest. 2007; 117:1902–1913. [PubMed: 17557120]
17. Hanayama R, Nagata S. Impaired involution of mammary glands in the absence of milk fat globule EGF factor 8. Proc Natl Acad Sci U S A. 2005; 102:16886–16891. [PubMed: 16275924]
18. Miksa M, Wu R, Dong W, Komura H, Amin D, Ji Y, Wang Z, Wang H, Ravikumar TS, Tracey KJ, Wang P. Immature dendritic cell-derived exosomes rescue septic animals via milk fat globule epidermal growth factor-factor VIII. J Immunol. 2009; 183:5983–5990. [PubMed: 19812188]
19. Ait-Oufella H, Kinugawa K, Zoll J, Simon T, Boddaert J, Heeneman S, Blanc-Brude O, Barateau V, Potteaux S, Merval R, Esposito B, Teissier E, Daemen MJ, Lesèche G, Boulanger C, Tedgui A, Mallat Z. Lactadherin deficiency leads to apoptotic cell accumulation and accelerated atherosclerosis in mice. Circulation. 2007; 115:2168–2177. [PubMed: 17420351]
20. Boddaert J, Kinugawa K, Lambert JC, Boukhtouche F, Zoll J, Merval R, Blanc-Brude O, Mann D, Berr C, Vilar J, Garabedian B, Journiac N, Charue D, Silvestre JS, Duyckaerts C, Amouyel P, Mariani J, Tedgui A, Mallat Z. Evidence of a role for lactadherin in Alzheimer's disease. Am J Pathol. 2007; 170:921–929. [PubMed: 17322377]
21. Silvestre JS, Théry C, Hamard G, Boddaert J, Aguilar B, Delcayre A, Houbron C, Tamarat R, Blanc-Brude O, Heeneman S, Clergue M, Duriez M, Merval R, Lévy B, Tedgui A, Amigorena S, Mallat Z. Lactoadherin promotes VEGF-dependent neovascularization. Nat Med. 2005; 11:499–506. [PubMed: 15834428]
22. Ensslin MA, Shur BD. The EGF repeat and discoidin domain protein, SED1/MFG-E8, is required for mammary gland branching morphogenesis. Proc Natl Acad Sci U S A. 2007; 104:2715–2720. [PubMed: 17299048]
23. Ensslin MA, Shur BD. Identification of mouse sperm SED1, a bimotif EGF repeat and discoidin-domain protein involved in sperm-egg binding. Cell. 2003; 114:405–417. [PubMed: 12941270]
24. Atabai K, Jame S, Azhar N, Kuo A, Lam M, McKleroy W, Dehart G, Rahman S, Xia DD, Melton AC, Wolters P, Emson CL, Turner SM, Werb Z, Sheppard D. Mfge8 diminishes the severity of tissue fibrosis in mice by binding and targeting collagen for uptake by macrophages. J Clin Invest. 2009; 119:3713–3722. [PubMed: 19884654]
25. Neutzner M, Lopez T, Feng X, Bergmann-Leitner ES, Leitner WW, Udey MC. MFG-E8/Lactadherin Promotes Tumor Growth in an Angiogenesis-Dependent Transgenic Mouse Model of Multistage Carcinogenesis. Cancer Res. 2007; 67:6777–6785. [PubMed: 17638889]
26. Lin MI, Yu J, Murata T, Sessa WC. Caveolin-1-deficient mice have increased tumor microvascular permeability, angiogenesis, and growth. Cancer Res. 2007; 67:2849–2856. [PubMed: 17363608]
27. Connor KM, Krah NM, Dennison RJ, Aderman CM, Chen J, Guerin KI, Sapieha P, Stahl A, Willett KL, Smith LE. Quantification of oxygen-induced retinopathy in the mouse: a model of vessel loss, vessel regrowth and pathological angiogenesis. Nat Protoc. 2009; 4:1565–1573. [PubMed: 19816419]
28. Hirschi KK, Rohovsky SA, D'Amore PA. PDGF, TGF-beta, and heterotypic cell-cell interactions mediate endothelial cell-induced recruitment of 10T1/2 cells and their differentiation to a smooth muscle fate. J Cell Biol. 1998; 141:805–814. [PubMed: 9566978]
29. Brachvogel B, Pausch F, Farlie P, Gaipl U, Etich J, Zhou Z, Cameron T, von der Mark K, Bateman JF, Pöschl E. Isolated Anxa5+/Sca-1+ perivascular cells from mouse meningeal vasculature retain their perivascular phenotype on vito and in vivo. Experiment Cell Research. 2007; 313:2730–2743.
30. Darland DC, D'Amore PA. TGF beta is required for the formation of capillary-like structures in three-dimensional cocultures of 10T1/2 and endothelial cells. Angiogenesis. 2001; 4:11–20. [PubMed: 11824373]
31. Au P, Tam J, Duda DG, Lin PC, Munn LL, Fukumura D, Jain RK. Paradoxical effects of PDGF-BB overexpression in endothelial cells on engineered blood vessels in vivo. Am J Pathol. 2009; 175:294–302. [PubMed: 19477947]

32. Zhang F, Tang Z, Hou X, Lennartsson J, Li Y, Koch AW, Scotney P, Lee C, Arjunan P, Dong L, Kumar A, Rissanen TT, Wang B, Nagai N, Fons P, Fariss R, Zhang Y, Wawrousek E, Tansey G, Raber J, Fong GH, Ding H, Greenberg DA, Becker KG, Herbert JM, Nash A, Yla-Herttuala S, Cao Y, Watts RJ, Li X. VEGF-B is dispensable for blood vessel growth but critical for their survival, and VEGF-B targeting inhibits pathological angiogenasis. Proc Natl Acad Sci U S A. 2009; 106:6152–6157. [PubMed: 19369214]
33. Jiang J, Xia XB, Xu HZ, Xiong Y, Song WT, Xiong SQ, Li Y. Inhibition of Retinal Neovascularization by Gene Transfer of small Interfering RNA Targeting HIF-1a and VEGF. J Cell Physiol. 2009; 218:66–74. [PubMed: 18767037]
34. Wilkinson-Berka JL, Jones D, Taylor G, Jaworski K, Kelly DJ, Ludbrook SB, Willette RN, Kumar S, Gilbert RE. SB-267268, a nonpeptidic antagonist of $\alpha_v\beta_3$ and $\alpha_v\beta_5$ integrins, reduces angiogenesis and VEGF expression in a mouse model of retinopathy of prematurity. Invest Ophthalmol Vis Sci. 2006; 47:1600–1605. [PubMed: 16565398]
35. Economopoulou M, Bdeir K, Cines DB, Fogt F, Bdeir Y, Lubkowski J, Lu W, Preissner KT, Hammes HP, Chavakis T. Inhibition of pathologic retinal neovascularization by alpha-defensins. Blood. 2005; 106:3831–3838. [PubMed: 16123222]
36. Stubbs JD, Lekutis C, Singer KL, Bui A, Yuzuki D, Srinivasan U, Parry G. cDNA cloning of a mouse mammary epithelial cell surface protein reveals the existence of epidermal growth factor-like domains linked to factor VIII-like sequences. Proc Natl Acad Sci U S A. 1990; 87:8417–8421. [PubMed: 2122462]
37. Ogura K, Nara K, Watanabe Y, Kohno K, Tai T, Sanai Y. Cloning and expression of cDNA for O-acetylation of GD3 ganglioside. Biochem Biophys Res Commun. 1993; 225:932–938. [PubMed: 8780713]
38. Andersen MH, Berglund L, Rasmussen JT, Petersen TE. Bovine PAS-6/7 binds alpha v beta 5 integrins and anionic phospholipids through two domains. Biochemistry. 1997; 36:5441–5446. [PubMed: 9154926]
39. Shao C, Novakovic VA, Head JF, Seaton BA, Gilbert GE. Crystal structure of lactadherin C2 domain at 1.7A resolution with mutational and computational analyses of its membrane-binding motif. J Biol Chem. 2008; 283:7230–7241. [PubMed: 18160406]
40. Jinushi M, Nakazaki Y, Carrasco DR, Draganov D, Souders N, Johnson M, Mihm MC, Dranoff G. Milk fat globule EGF-8 promotes melanoma progression through coordinated Akt and twist signaling in the tumor microenvironment. Cancer Res. 2008; 68:8889–8898. [PubMed: 18974133]
41. Fu Z, Wang M, Gucek M, Zhang J, Wu J, Jiang L, Monticone RE, Khazan B, Telljohann R, Mattison J, Sheng S, Cole RN, Spinetti G, Pintus G, Liu L, Kolodgie FD, Virmani R, Spurgeon H, Ingram DK, Everett AD, Lakatta EG, Van Eyk JEs. Milk fat globule protein epidermal growth factor-8: a pivotal relay element within the angiotensin II and monocyte chemoattractant protein-1 signaling cascade mediating vascular smooth muscle cells invasion. Circ Res. 2009; 104:1337–1346. [PubMed: 19443842]
42. Jinushi M, Sato M, Kanamoto A, Itoh A, Nagai S, Koyasu S, Dranoff G, Tahara H. Milk fat globule epidermal growth factor-8 blockade triggers tumor destruction through coordinated cell-autonomous and immune-mediated mechanisms. J Exp Med. 2009; 206:1317–1326. [PubMed: 19433619]
43. Fens MH, Mastrobattista E, de Graaff AM, Flesch FM, Ultee A, Rasmussen JT, Molema G, Storm G, Schiffelers RM. Angiogenic endothelium shows lactadherin-dependent phagocytosis of aged erythrocytes and apoptotic cells. Blood. 2008; 111:4542–4550. [PubMed: 18292292]
44. Ozerdem U, Stallcup WB. Pathological angiogenesis is reduced by targeting pericytes via the NG2 proteoglycan. Angiogenesis. 2004; 7:269–276. [PubMed: 15609081]
45. Hammes HP, Lin J, Wagner P, Feng Y, Vom Hagen F, Krzizok T, Renner O, Breier G, Brownlee M, Deutsch U. Pericytes and the pathogenesis of diabetic retinopathy. Diabetes. 2002; 51:3107–3112. [PubMed: 12351455]
46. Davies MH, Eubanks JP, Powers MR. Microglia and macrophages are increased in response to ischemia-induced retinopathy in the mouse retina. Mol Vis. 2006; 12:467–477. [PubMed: 16710171]

47. Reznikoff CA, Brankow DW, Heidelberger C. Establishment and characterization of a cloned line of C3H mouse embryo cells sensitive to postconfluence inhibition of division. Cancer Res. 1973; 33:3231–3238. [PubMed: 4357355]

48. Hart JR, Liao L, Ueno L, Yates JR 3rd, Vogt PK. Protein expression profiles of C3H 10T1/2 murine fibroblasts and of isogenic cells transformed by the H1047R mutant of phosphoinositide 3-kinase (PI3K). Cell Cycle. 2011; 10:971–976. [PubMed: 21350335]

49. Joo SY, Cho KA, Jung YJ, Kim HS, Park SY, Choi YB, Hong KM, Woo SY, Seoh JY, Cho SJ, Ryu KH. Mesenchymal stromal cells inhibit graft-versus-host disease of mice in a dose-dependent manner. Cytotherapy. 2010; 12:361–370. [PubMed: 20078382]

50. Kurzen H, Manns S, Dandekar G, Schmidt T, Prätzel S, Kräling BM. Tightening of endothelial cell contacts: a physiologic response to cocultures with smooth-muscle-like 10T1/2 cells. J Invest Dermatol. 2002; 119:143–153. [PubMed: 12164937]

51. Dhar K, Dhar G, Majumder M, Haque I, Mehta S, Van Veldhuizen PJ, Banerjee SK, Banerjee S. Tumor cell-derived PDGF-B potentiates mouse mesenchymal stem cells-pericytes transition and recruitment through an interaction with NRP-1. Mol Cancer. 2010; 9:209. [PubMed: 20687910]

52. Zemskov EA, Loukinova E, Mikhailenko I, Coleman RA, Strickland DK, Belkin AM. Regulation of platelet-derived growth factor receptor function by integrin-associated cell surface transglutaminase. J Biol Chem. 2009; 284:16693–16703. [PubMed: 19386600]

53. Bu HF, Zuo XL, Wang X, Ensslin MA, Koti V, Hsueh W, Raymond AS, Shur BD, Tan XD. Milk fat globule-EGF factor 8/lactadherin plays a crucial role in maintenance and repair of murine intestinal epithelium. J Clin Invest. 2007; 117:3673–3683. [PubMed: 18008006]

54. Somanath PR, Malinin NL, Byzova TV. Cooperation between integrin alphavbeta3 and VEGFR2 in angiogenesis. Angiogenesis. 2009; 12:177–185. [PubMed: 19267251]

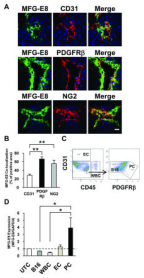

Figure 1.

MFG-E8 is produced by, and localizes in close proximity to, pericytes in tumors. A, Localization of MFG-E8 in relationship to EC (CD31+) and PC (PDGFRβ+, NG2+) in 1 cm B16 melanomas using confocal microscopy (Bar = 20 μ). B, Quantification of co-localization of MFG-E8 with CD31, PDGFRβ and NG2 in digitized confocal microscopic images using Image J (***p*<0.01; n=10 sections from n=3 tumors). C, Isolation of flow cytometry-sorted melanoma cells (CD31− CD45− PDGFRβ−), leukocytes (WBC; CD45+ CD31−), EC (CD45− CD31+) and PC (CD45− CD31− PDGFRβ+) from B16 melanoma cells after dispase digestion. D, Quantification of MFG-E8 mRNA levels in tumor cell subpopulations using quantitative RT-PCR. Data are expressed relative to MFG-E8 mRNA levels in unfractionated tumor cells (UTC) (**p*<0.05; Values determined in 4 independent experiments).

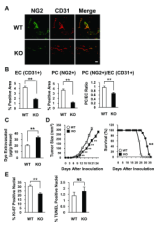

Figure 2.

Characterization of tumor-associated vessels and tumor progression in B16 melanomas implanted into syngeneic MFG-E8 knockout mice. A, Immunofluorescence confocal photomicrographs depicting vessel-associated NG2 and CD31 distribution in 1 cm melanomas (Bar =100 μ). B, Quantification of extent of vascularization (EC, PC area), and PC coverage (PC/EC ratio) in 1 cm B16 melanomas growing in WT and MFG-E8 KO mice (**p<0.01; values determined in 10 random confocal microscopic fields in n=4 tumors per genotype). C, Quantification of vessel permeability (Evans blue dye extravasation) in 1 cm B16 melanomas growing in WT and MFG-E8 KO mice (**p<0.01; n=10–12 mice in each group). D, Retardation of tumor growth and prolongation of survival in MFG-E8 KO mice after implantation of B16 melanoma cells (*p<0.05; **p<0.01; data are representative of n=3 experiments (n=10 mice in each group)). E, Diminished proliferation of B16 cells without increased apoptosis in MFG-E8 KO as compared with WT mice (**p<0.01; values determined in 10 random microscopic fields in n=3 tumors per genotype, NS = not significant).

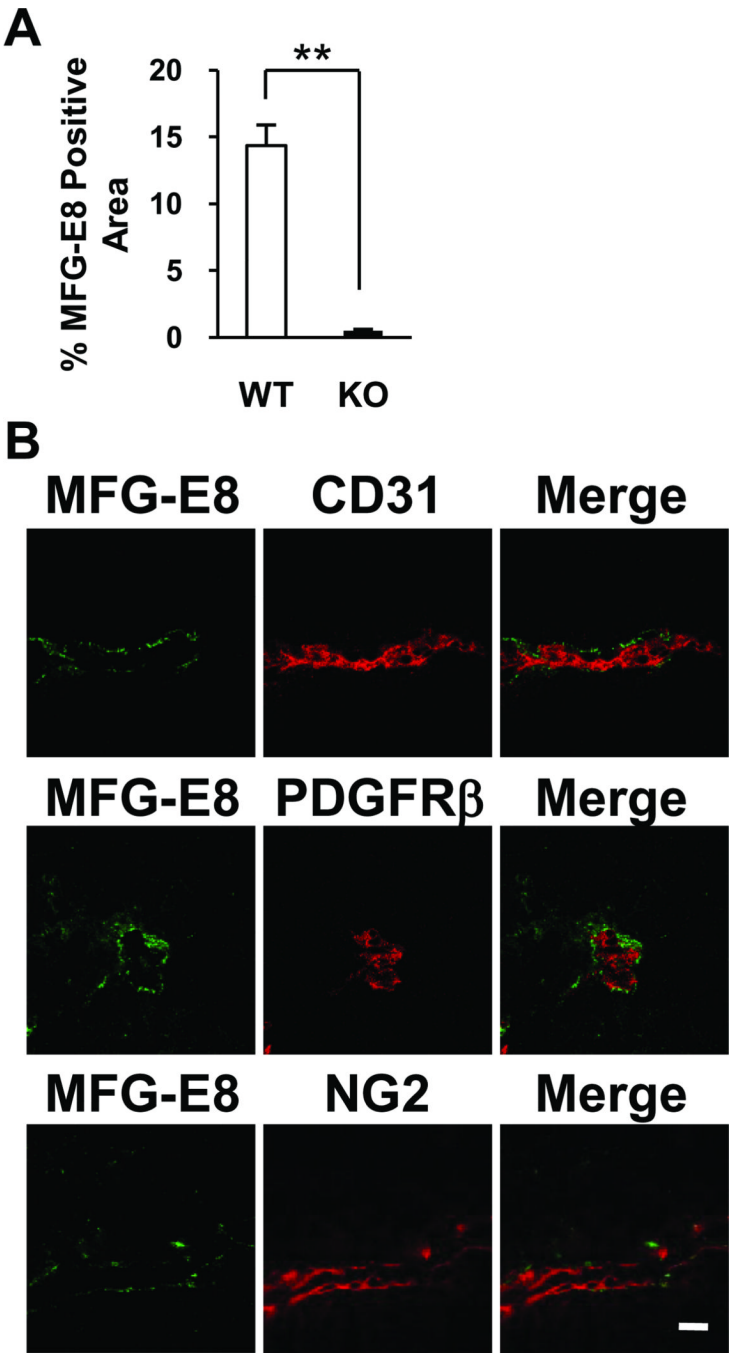

Figure 3.

In situ localization and quantification of melanoma cell-derived MFG-E8 in tumors in MFG-E8 knockout mice. A, Drastic reduction of MFG-E8 accumulation in B16 tumors growing in MFG-E8 KO compared to WT mice (**p<0.01; values determined in 10 random confocal microscopic fields from n=3 tumors). B, Distribution of melanoma cell-derived MFG-E8 in relationship to EC (CD31+) and PC (PDGFRβ+, NG2+) in 1 cm B16 melanomas in MFG-E8 KO mice demonstrated via confocal immunofluorescnce microscopy (Bar = 20μ).

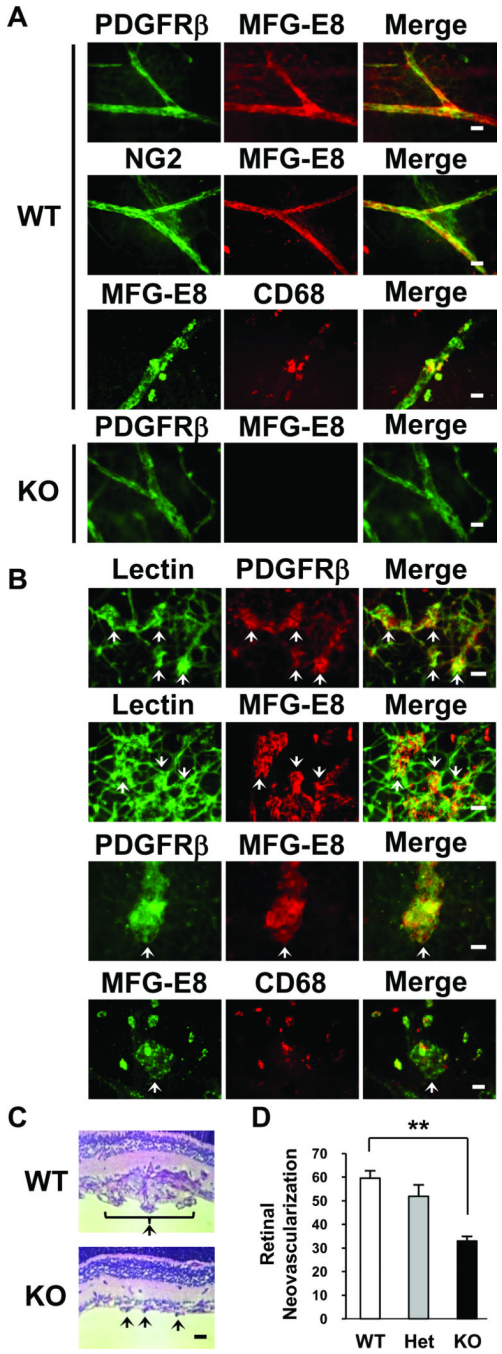

Figure 4.

Characterization of the role of MFG-E8 in angiogenesis induced during oxygen-induced retinopathy in mice. A, Localization of MFG-E8 in relationship to PC (PDGFRβ+, NG2+) in normal retina from WT and MFG-E8 KO mice using rabbit anti-mouse MFG-E8 polyclonal Ab (Bar = 20μ). B, Fluorescence photomicrographs depicting localization of MFG-E8 in relationship to neovascular tufts (arrows, lectin+), PC (PDGFRβ+) and macrophages (CD68+) (day P17 after initiation of hyperoxia in WT mice, Bar = 50 μ). C, Photomicrograph of neovascular tufts (arrows) extending into the vitreous in littermate control and MFG-E8 KO mice on day P17 (formalin-fixed, paraffin-embedded sections stained with periodic acid Schiff (PAS) and hematoxylin). D, Quantification of retinal

neovascularization which is the number of vessel-associated nuclei above the inner limiting membrane into the vitreous on day P17 after initiation of oxygen-induced retinopathy protocol (**p<0.01; n= 16, 12 and 16 mice for WT, heterozygous (Het) and MFG-E8 KO mice, respectively).

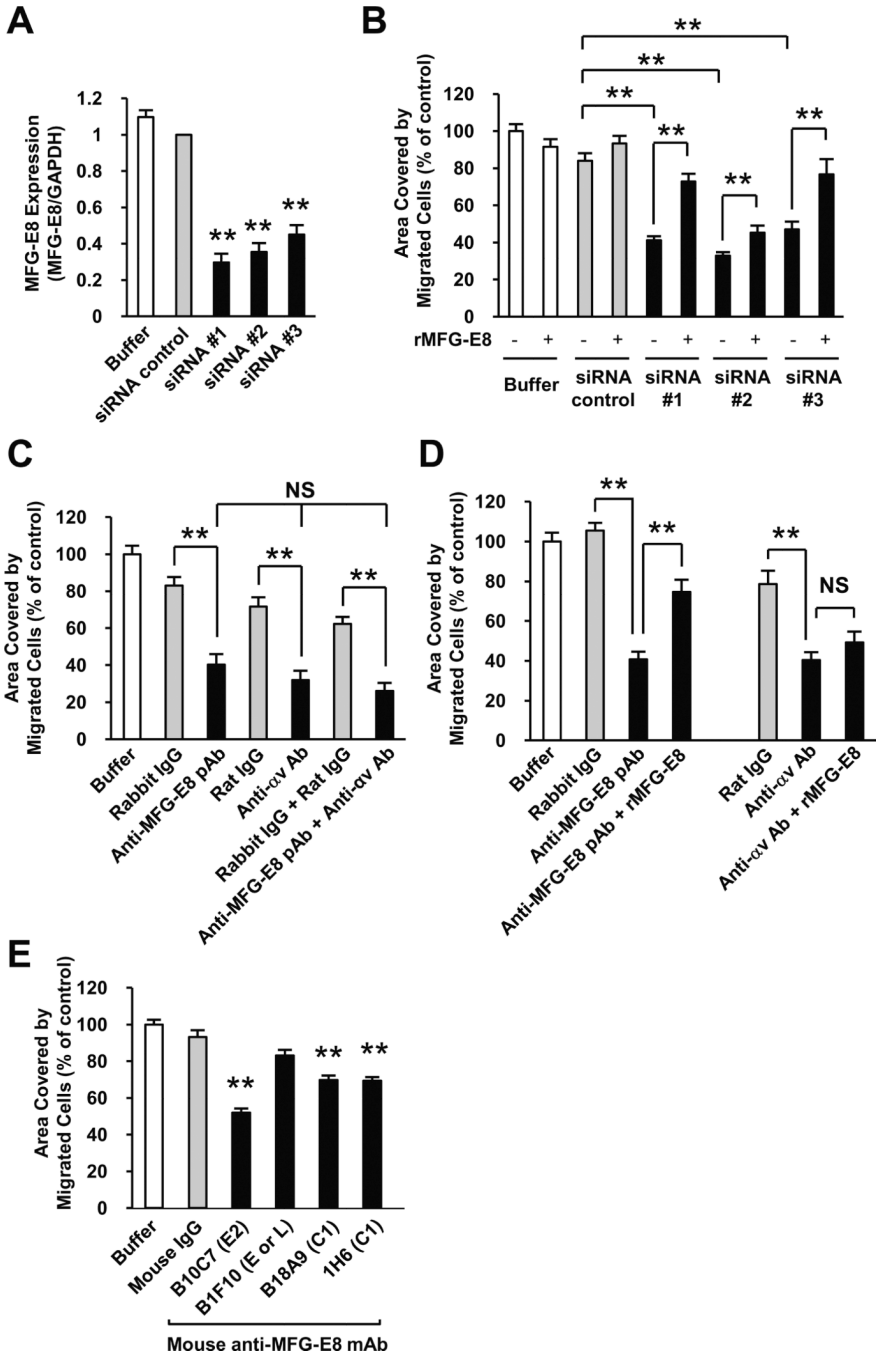

Figure 5.

Inhibition of 10T1/2 cell migration by MFG-E8 siRNAs, or by anti-MFG-E8 antibodies in vitro. A, siRNA-induced inhibition of MFG-E8 mRNA expression by 10T1/2 cells assessed by quantitative RT-PCR 48 hours after transfection and immediately prior to the migration assay (**p<0.01 relative to siRNA control; Values determined in 6 independent experiments). B, Migration of control and MFG-E8 knockdown 10T1/2 cells by siRNA, and reversal of effect by addition of recombinant MFG-E8 protein (100 ng/ml). 10T1/2 cells adherent to the bottom surfaces of FluoroBlok™ filters 4 hours after initiation of PDGF-B-induced migration was quantified using ImageJ (*p<0.05; **p< 0.01; Values determined in 20 fields in n=2 experiments). C, Comparison of inhibitory effects of anti-MFG-E8 pAb,

anti-αv mAb, and both anti-MFG-E8 pAb and anti-αv mAb (all at 20 μg/ml) on PDGF-B-induced migration in FluoroBlok™ assay at 4 hours (**p< 0.01; Values determined in 16 fields in n=2 experiments, NS = not significant). D, Selective reversal of inhibitory effects of anti-MFG-E8 pAb (20 μg/ml), but not anti-αv mAb (20 μg/ml) by addition of recombinant MFG-E8 protein (*p< 0.05, **p< 0.01; Values determined in 16 fields in n=2 experiments, NS = not significant). E, Comparison of inhibitory effects of anti-MFG-E8 mAb (20 μg/ml) reactive with various domains on PDGF-B-induced 10T1/2 PC migration at 4 hours (**p< 0.01 relative to mouse IgG control, Values determined in 30 fields in n=3 experiments).

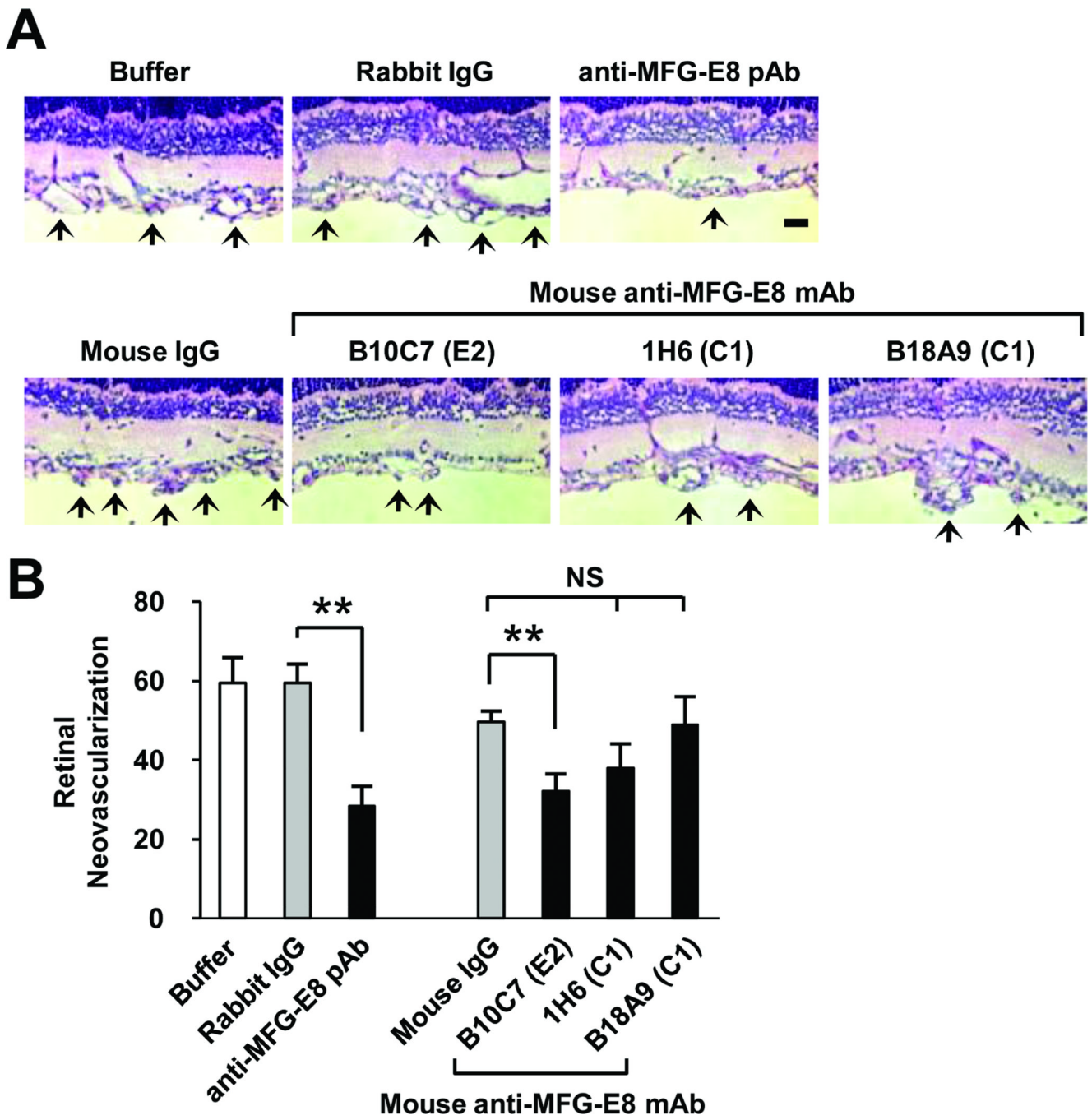

Figure 6.

Inhibition of pathologic angiogenesis occurring secondary to oxygen induced retinopathy by anti-MFG-E8 antibodies. A, Representative photomicrographs of histologic sections from retinas in WT mice at day P17 in the oxygen induced retinopathy protocol (arrows highlight neovascularization). Mice were treated with 50 μg of the indicated Ab or control IgG on days P12, 14 and 16. B, Quantification of retinal neovascularization which is the number of vessel-associated nuclei above the inner limiting membrane into the vitreous on day P17 after initiation of oxygen-induced retinopathy protocol (**$p<0.01$; n=4–5 mice per treatment).